AD-A076 099 NEW YORK UNIV N Y DEPT OF PHYSICS F/G 7/4

STUDY OF COLLISIONAL REDISTRIBUTION USING TWO-PHOTON ABSORPTION--ETC(U)

SEP 79 P R BERMAN, P F LIAO, J E BJORKHOLM N00014-77-C-0553

UNCLASSIFIED NL

1 OF 1

AD A 076099

END

DATE FILMED

12-79

DDC

To appear in Phys. Rev. A

AD A076099

DDC FILE COPY

LEVEL II

6

STUDY OF COLLISIONAL REDISTRIBUTION USING TWO-PHOTON ABSORPTION WITH A NEARLY RESONANT INTERMEDIATE STATE

12

by

P. F. Liao [redacted] J. E. Bjorkholm
Bell Telephone Laboratories
Holmdel, New Jersey 07733

and

10 P. R. Berman
Physics Department, New York University
New York, New York 10003

12 14

11 Sep 79

ABSTRACT

We report studies of collision-induced features of the $3S_{1/2} \rightarrow 3P_{1/2} \rightarrow 4D_{3/2}$ two-photon absorption in atomic sodium vapor undergoing collisions with several rare gas perturbers. The results yield the collisional redistribution function which describes the nonresonant excitation of the $3P_{1/2}$ intermediate state. Good agreement with theory is obtained only if effects of $3P_{1/2} \leftrightarrow 3P_{3/2}$ state-changing collisions are included in the calculations. Results are used to obtain a value for a pressure broadening coefficient in the Na-Kr system.

yields

in equilibrium with

Supported by the U.S. Office of Naval Research under Contract No. N00014-77-C-0553

15

September 1979

406 850

79 09 17 082

mt

STUDY OF COLLISIONAL REDISTRIBUTION USING TWO-PHOTON ABSORPTION WITH A NEARLY RESONANT INTERMEDIATE STATE

by

P. F. Liao and J. E. Bjorkholm
Bell Telephone Laboratories
Holmdel, New Jersey 07733

and

P. R. Berman
Physics Department, New York University
New York, New York 10003

The spectrum of light scattered by an atomic vapor illuminated by nearly resonant radiation has attracted considerable interest[1-6]. Experiments have been reported in which narrow-band laser radiation is scattered by an atomic or molecular vapor[3-6]. For a two-level system, low laser intensities, and radiation tuned outside the Doppler width of the transition, the scattered light spectrum is found to contain two components. One component is centered at the incident laser frequency and is due to Rayleigh scattering. The second component is found to be centered at the frequency of the atomic resonance line and has a pressure-dependent intensity which vanishes in the absence of collisions. The appearance of this component at the frequency of the resonance transition is known as collisional redistribution. In this paper we report measurements of the collisional redistribution function which are made in absorption rather than in emission. Two-photon absorption spectra are obtained with two cw dye lasers operating at different frequencies. The absorption is measured

This paper has been submitted to Physical Review.

as the frequency of one laser is scanned. The resulting lineshape contains two components which are similar in nature to the two components found in emission experiments. One component is a collision-induced signal corresponding to the collisional redistribution; it results from the collisionally aided excitation of the nonresonant intermediate state followed by the subsequent absorption of a photon which causes a transition to the final state. The second component is due to direct two-photon transitions from the ground state to the excited state and is analogous to the Rayleigh scattering observed in emission. The redistribution process which we observe is important to problems of radiative energy transport[7]. It must also be included to correctly analyze lineshape experiments which probe velocity-changing collisions[8,9].

The theory of spectral redistribution of scattered light in the impact approximation is well developed[1,2,10]. In this approximation the detuning of the incident light from the resonance must be much less than $2\pi/\tau_c$, where τ_c is the duration of a collision. Recent experiments have investigated various aspects of collisional redistribution. The first experimental evidence appears to have been obtained by Rousseau et al.[5], although they were not able to completely resolve the various components. More recently the resonance scattering from sodium in high pressure helium was found to exhibit complete collisional redistribution[6]. Carlsten et al.[3,4]

have made investigations in the regime where the laser detuning is large and the impact approximation is not valid. In our work we use two-photon spectroscopy to examine in detail the redistribution function in the impact regime for sodium atoms undergoing collisions with rare gas perturbers. To our knowledge this work represents the only study which measures both the shape and amplitude of the collisional redistribution; furthermore, it demonstrates the importance of state-changing collisions on the redistribution. The theory of the effect of collisions on two-photon lineshapes has been discussed (see reference 10 and references therein) and our results are found to be in good agreement with these theories if the theory is extended to include the effects of fine-structure state-changing collisions. An experiment which demonstrated the different time dependences of the two components we have observed in two-photon absorption has been reported by Grischkowsky[11].

Our experimental apparatus[12] consists of two cw single-mode frequency-stabilized dye lasers (Coherent 599) whose unfocused output beams were passed in opposing directions through a 1 cm long cell at 200°C containing sodium vapor. Both laser beams were linearly polarized in the same direction and had intensities of about 1 W/cm^2. The sodium vapor density was maintained at approximately 10^{11} cm^{-3}. The pressure of rare gas introduced into the cell was measured with a capacitance manometer. One dye laser was held at a fixed frequency Ω nearly resonant with but outside the Doppler width of the $3S_{1/2} \rightarrow 3P_{1/2}$ transition

($\sim$ 5896Å) while the other frequency Ω' ($\sim$ 5682Å) was scanned to complete transitions to the $4D_{3/2}$ state. Transitions to $4D_{5/2}$ are extremely weak and can be neglected in comparison to those to $4D_{3/2}$ since the nearly resonant $3P_{1/2}$ intermediate state enhances only transitions to $4D_{3/2}$. The population of the $4D_{3/2}$ state is monitored by observing the $\sim$ 330 nm fluorescence which occurs when the $4D_{3/2}$ state decays via the 4P state back to the ground state.

Figure 1 illustrates spectra obtained in our experiment for various pressures of neon gas. Similar data was obtained with helium and krypton. The fixed frequency laser is set 4.0 GHz below the $3S_{1/2}$ (F=2) $\rightarrow 3P_{1/2}$ transition frequency. Three distinct lines are readily identified. The two narrow lines correspond to direct two-photon transitions from the two hyperfine states of the ground state to the $4D_{3/2}$ final state. These lines are nearly Doppler-free because the excitation is made with oppositely propagating waves with nearly the same frequency[12]. The broad line is the collision-induced signal. As shown in Fig. 1, it vanishes in the absence of buffer gas; this collisional redistribution signal increases as the buffer gas pressure increases.

The source of the redistribution signal is collisionally-induced population of the $3P_{1/2}$ state. Collisions can supply the energy to compensate for the mismatch between $\hbar\Omega$

and the energy of the resonant transition. The excitation of the intermediate state is essentially velocity independent and hence the redistribution component is broad with a width which is dominated by the Doppler width of the $3P_{1/2} - 4D_{3/2}$ transition. For a more detailed discussion of the origin of the redistribution component, see, for example, reference 10 or 13.

Collision-induced transfer of population between various sublevels within the $3P_{1/2}$ state does not affect our signals because with linearly polarized light the total excitation transition rate from each sublevel to the $4D_{3/2}$ level is the same. The field at Ω can create coherence between the $F = 2$, $M_F = \pm 1$ and $F = 1$, $M_F = \pm 1$ levels of the $3P_{1/2}$ state but these coherences contribute negligibly to our signal. Thus it is only the total population of the $3P_{1/2}$ state that enters in calculating the redistribution signal.

For a three-level system the lineshapes and relative amplitudes of the redistribution and two-photon resonances can be approximated by the following expressions[10]. The narrow two-photon resonance is proportional to

$$\rho_{33} \approx C \frac{k}{|k'-k|} \left(\frac{ku}{\Delta}\right)^2 \quad z_i\left(\frac{i\tilde{\eta}_{13}}{|k'-k|u}\right) , \qquad (1)$$

and the redistribution term is proportional to

$$\rho_{33} \approx C\left(\frac{k}{k'}\right) \left(\frac{ku}{\Delta}\right)^2 \left(\frac{2\tilde{\gamma}_{12}}{\gamma_{2eff}} - 1\right) \quad z_i\left(\frac{i\tilde{\eta}_{23}}{k'u}\right) , \qquad (2)$$

where $\tilde{\eta}_{13} = \tilde{\gamma}_{13} + i\,(\Delta + \Delta')$, $\tilde{\eta}_{23} = \tilde{\gamma}_{23} + i\Delta'$ and $\Delta = \Omega - \omega$, $\Delta' = \Omega' - \omega'$. The angular frequencies ω and ω' are the transition

frequencies of the ground to intermediate and intermediate to final state respectively. The wave vectors are $k' = \Omega'/c$ and $k = \Omega/c$, the subscripts 1, 2, and 3 refer to the ground, intermediate, and final states respectively, and u is the most probable speed. The decay rates $\tilde{\gamma}_{ij}$ are the phenomenológical decay constants of the density matrix elements ρ_{ij} and include the effects of phase-changing collisions. The quantity $z_i\ (u)$ is the imaginary part of the plasma dispersion function defined in appendix A, and C is a constant of proportionality[14]. One may deduce the following useful information from these formulas: 1) the two-photon resonances are narrow, 2) the redistribution peak (centered at $\Delta' = 0$) is Doppler broadened, 3) the ratio of the amplitudes of the braod to narrow resonances is independent of Δ and depends on pressure only, and 4) the amplitude of the redistribution term vanishes in the limit of zero pressure where $2\tilde{\gamma}_{12} = \gamma_{2eff}$.

The effect of fine-structure state-changing collisions is quite important as it modifies the amplitude of the collisional redistribution signals by a significant amount. The $3P_{1/2} \leftrightarrow 3P_{3/2}$ state-changing collisions must be included since they give rise to appreciable relaxation for atoms in the $3P_{1/2}$ state. By solving the rate equations for the steady-state we find these collisions produce an effective decay rate for the intermediate state (see Appendix B) of

$$\gamma_{2eff} = \gamma_2 \frac{\gamma_2 + 1.5\ \gamma_t}{\gamma_2 + 0.5\ \gamma_t} \qquad (3)$$

where γ_2 is the natural decay rate of the $3P_{1/2}$ state equal to 6.3×10^7 sec^{-1} and γ_t is the rate of transfer for $3P_{1/2} \rightarrow 3P_{3/2}$. This rate is proportional to pressure and is calculated from measured cross sections[15,16]. The effect of state-changing collisions on collisional redistribution in emission has recently been theoretically treated by Cooper and Ballagh[17].

Equations (1) and (2) are valid in the impact limit with $|\Delta| >> ku$. To achieve greater accuracy in our calculations we have used more general expressions given in the Appendix A. This Appendix also contains a method for including the contributions of both hyperfine ground-state levels.

The points in Fig. 1 show our theoretically-calculated values for the lineshape. The relative amplitudes of the two narrow two-photon transitions were adjusted to exactly match the experimental data. This adjustment was required because of optical pumping effects which cause the population of the ground hyperfine states to vary slightly with pressure and laser intensity. Except for this adjustment no other free parameters are taken in the calculation. The values used for the collisional rate coefficients are given in Table 1 and are taken from the literature. The theory accurately predicts the amplitudes and widths of lines in the observed spectra at all pressures. To illustrate the importance of accounting for the fine-structure state-changing collisions, we indicate in Fig. 2 the theoretical result at 10.8 Torr of neon that would be obtained if these state changes were neglected. The effect of the state-changing collisions is to distribute the

energy among all the fine-structure states with the result that the redistribution peak is lowered by a factor of 2.5. The correction varies up to a factor of 3 depending on the pressure, and for all pressures greater than about 1 Torr, gives rise to a substantial modification to the theory.

The results with other rare gases such as helium and krypton were similar to those obtained with neon. Figure 3 shows some typical lineshapes obtained with helium and krypton. The agreement for collisions with helium is excellent with all relaxation rates calculated from published values. To our knowledge no published values for the pressure dependence of $\tilde{\gamma}_{12}$ exists for the sodium-krypton system so the theoretical points for krypton in Figure 3 represent a fit to our experimental data. The pressure broadening coefficient obtained by this fit is $\frac{1}{2\pi}\left(d\tilde{\gamma}_{12}/dP\right) = 12.0 \pm 2$ MHz/Torr.

The dependence of the amplitude of the redistributed component on laser detuning is shown in Fig. 4. The solid line is theoretical and assumes contributions from both ground hyperfine levels but does not account for optical pumping. The agreement is excellent. The ratio of the redistribution amplitude to the amplitudes of the narrow two-photon resonances was found to be essentially independent of detuning in accordance with theory.

We have experimentally verified the predictions of the theory of collisional redistribution and two-photon absorption in the impact regime. Comparisons of the experimental lineshapes reveal good agreement with a theory having essentially no adjustable parameters. The importance of state-changing collisions on the redistribution has been demonstrated for the first time. We have used our measurements to obtain the broadening coefficient of the sodium resonance line for collisions with krypton. It should be noted that essentially all the relaxation parameters of an atomic system could have been obtained by these experiments. The widths of the two-photon resonances yield $\tilde{\gamma}_{13}$, the width of the redistribution component yields $\tilde{\gamma}_{23}$, and its amplitude is dependent on $\tilde{\gamma}_{12}$ and γ_t. The good agreement between the amplitudes and widths of the resonances in our experiment with the theory may be taken as confirmation of the broadening coefficients used in our calculation.

The research of one author (PRB) was partially supported by the Office of Naval Research.

APPENDIX A

For the pump field strength $(\chi/ku) = 0.018$ [χ = Rabi frequency at zero detuning] and detuning $|\Delta|/ku = 4.0$ used in this experiment, the line shape is adequately described by the perturbation theory of Reference 10. The result, derived for a three-level system, is

$$I = I_{TQ} + I_{SW} \tag{A-1}$$

where

$$I_{TQ} = -\frac{C}{\sqrt{\pi}}\frac{k}{k'}\frac{k}{(k'-k)}\,\mathrm{Im}\int\frac{W_o(X)\,dX}{\left[\frac{i\,\tilde{\Gamma}_{12}}{ku}+X\right]\left[\frac{i\,\tilde{\Gamma}_{23}}{k'u}-X\right]\left[\frac{i\,\tilde{\Gamma}_{13}}{(k'-k)u}-X\right]} \tag{A-2}$$

and

$$I_{SW} = \frac{2C}{\sqrt{\pi}}\left(\frac{k}{k'}\right)\left(\frac{\tilde{\gamma}_{23}}{k'u}\right)\iint\frac{\tilde{\gamma}_{12}\,W_o(X)G_{22}(X+X')\,dX\,dX'}{\left|\frac{i\,\tilde{\Gamma}_{12}}{ku}+X\right|^2\left|\frac{i\,\tilde{\Gamma}_{23}}{k'u}-X'\right|^2} \tag{A-3}$$

represent the "two-quantum and "stepwise" contributions to the line shape. The variables appearing in Eqs. (A-1) and (A-2) are defined as follows: C is a constant proportional to the pump field intensity,

$$\tilde{\Pi}_{12} = \tilde{\gamma}_{12} + i\,\tilde{\Delta} \qquad \text{(A-4a)}$$

$$\tilde{\Pi}_{23} = \tilde{\gamma}_{23} + i\,\tilde{\Delta}' \qquad \text{(A-4b)}$$

$$\tilde{\Pi}_{13} = \tilde{\gamma}_{13} + i\,(\Delta+\Delta') \qquad \text{(A-4c)}$$

with tilde's indicating collisionally broadened and shifted values of the widths and detunings, the function

$$W_o(X) = \pi^{-1/2}\, e^{-X^2} \quad . \qquad \text{(A-5)}$$

is the thermal velocity distribution in dimensionless units, and $G_{22}(X \to X')$ is a propagator[10] accounting for velocity-changing collisions in level 2. Equations (A-2) and (A-3) can be evaluated in terms of Plasma Dispersion functions,[10] but asymptotic forms in the large detuning limit are more easily obtained from the integral expressions.

One sees immediately from Eq. (A-3) that the SW contribution depends on velocity-changing collisions through the propagator $G_{22}(X \to X')$. However, for large detunings $|\Delta|/ku >> 1$, the denominator $(i\,\tilde{\Pi}_{12}/ku + X)$ can be approximated by $\frac{i\Delta}{ku}$ over the range of X that contributes to the integral and the integral over X in Eq. (A-3) is easily evaluated using the relation[10]

$$\int G_{22}(X \to X') W_o(X)\, dX = W_o(X')/\gamma_{2eff} \quad , \qquad \text{(A-6)}$$

where γ_{2eff} is the effective lifetime of level 2. Equation (A-6) expresses the fact that collisions do not change an equilibrium distribution. Hence, one obtains a SW contribution

$$I_{SW} = 2C\left(\frac{k}{k'}\right)\left(\frac{\tilde{\gamma}_{12}}{\gamma_{2eff}}\right)\left(\frac{ku}{\Delta}\right)^2 Z_i\left(\frac{i\,\tilde{\Pi}_{23}}{k'u}\right) \quad , \qquad \text{(A-7)}$$

where $Z_i(\nu)$ is the imaginary part of the Plasma Dispersion function,

$$Z(\nu) = -\,\pi^{-1/2} \int e^{-X^2} (\nu \pm X)^{-1} dX$$

with $\mathrm{Im}(\nu) > 0$.

Corrections to Eq. (A-7) are of order $(ku/\Delta)^{-2}$ ≈ 0.06, and depend on the specific collision model adopted. In order to avoid specific models, we neglect all such corrections in this term. Consequently, the amplitude of the redistribution may be in error by an amount on the order of 6 percent. [Computer calculations using a fairly general collision model indicate that (A-7) underestimates I_{SW} by 2 to 8 percent.]

For the TQ contribution in the limit $|\Delta|/ku >> 1$, Eq. (A-2) can be evaluated numerically for all values of Δ'.

However, in the regions about the narrow resonance $\Delta' \simeq -\Delta$ and the broad one $\Delta' \simeq 0$, it suffices to use approximate forms. Near $\Delta' = -\Delta$, one finds, to order $(ku/\Delta)^2$,

$$I_{TQ} = \frac{Ck}{|k'-k|}\left(\frac{ku}{\Delta}\right)^2 z_i\left(\frac{i\,\tilde{\eta}_{13}}{|k'-k|u}\right)\left[1 + \left(\frac{ku}{\Delta}\right)^2 \alpha\left(\frac{\tilde{\gamma}_{13}}{|k'-k|u}\right)\right] \qquad \text{(A-8)}$$

for $\Delta' \simeq \Delta$,

where

$$\alpha(X) = 3X^2\left\{\left[X\, z_i(X)\right]^{-1} - 1\right\}$$

$$\sim \begin{cases} \frac{3}{2}\left(1 - \frac{2}{X^2}\right) & \text{for } X \gg 1 \\ 3\pi^{-1/2}\, X & \text{for } X \ll 1 \end{cases} \qquad \text{(A-9)}$$

Experimentally, $\tilde{\gamma}_{13}/(k'-k)u$ varies from 1.7 to 5.

Near $\Delta' = 0$, the term is

$$I_{TQ} = -\,C\left(\frac{k}{k'}\right)\left(\frac{ku}{\Delta}\right)^2 z_i\left(\frac{i\,\tilde{\eta}_{23}}{k'u}\right)\left[1 + \left(\frac{ku}{\Delta}\right)^2 \alpha\left(\frac{\tilde{\gamma}_{23}}{k'u}\right)\right] \qquad \text{(A-10)}$$

for $\Delta' \simeq 0$.

Since $\tilde{\gamma}_{23}/ku \lesssim 1$ and $|ku/\Delta| = 0.25$ for our experiment, the second term in square brackets represents a negligible correction and may be dropped.

Combining Eq. (A-8) and Eq. (A-7) the line shape near $\Delta' \simeq -\Delta$ is given by

$$I = C\left(\frac{ku}{\Delta}\right)^2\left[\frac{k}{k'-k}\, z_i\left(\frac{i\,\tilde{\eta}_{13}}{(k'-k)u}\right)\left[1 + \left(\frac{ku}{\Delta}\right)^2 \alpha\left(\frac{\tilde{\gamma}_{13}}{(k'-k)u}\right)\right] + 2\left\{\left(\frac{ku}{\Delta}\right)^2\right\} \frac{\tilde{\gamma}_{12}\,\tilde{\gamma}_{23}}{\gamma_{2eff}\; ku}\right]$$

(A-11)

where we have used $z_i\left(i\,\tilde{\eta}_{23}/k'u\right) \simeq \tilde{\gamma}_{23}\, k'u/\Delta^2$ in this region. Equation (A-11) gives values generally a few percent less than computer evaluation of Eqs. (A-2) and (A-3).

In the region $\Delta' \simeq 0$, one combines (A-10) and (A-7) to obtain the *redistribution resonance*

$$I = C\left(\frac{k}{k'}\right)\left\{\left(\frac{ku}{\Delta}\right)^2\right\}\left[\frac{2\tilde{\gamma}_{12}}{\gamma_{2eff}} - 1\right] z_i\left(\frac{i\,\tilde{\eta}_{23}}{k'u}\right) . \qquad \text{(A-12)}$$

In the actual experimental situation, there are two hyperfine levels in the ground state separated by 1.77 GHz. The total line shape depends on contributions from both of these levels. The detuning for transitions originating from the $F = 2$ state is Δ while that from the $F = 1$ state is Δ_2 where $\Delta_2/2\pi = \Delta/2\pi - 1.77$ GHz. The net modification of the line shape is the replacement of the factors $(ku/\Delta)^2$ appearing in curly brackets in Eqs. (A-11) and (A-12) by $(ku)^2(\Delta^{-2}+w\Delta_2^{-2})$, where w accounts for relative statistical weights and optical pumping of transitions originating from $F = 1$ versus those originating from $F = 2$. In fitting the data, w is the only adjustable parameter.

APPENDIX B

Derivation of γ_{2eff}

The influence of the $3P_{3/2}$ state collisionally coupled to the $3P_{1/2}$ intermediate state can be included without much difficulty. In the perturbation limit and the large pump detuning limit $|\Delta/ku| >> 1$, the steady state equations for the $P_{1/2}$ and $P_{3/2}$ population densities $n_{1/2}(v)$ and $n_{3/2}(v)$ for a ground state density N_o are

$$0 = -\gamma_2 n_{1/2} - \Gamma n_{1/2} + \Gamma' n_{3/2} + S \qquad \text{(B-1a)}$$

$$0 = -\gamma_2 n_{3/2} - \Gamma' n_{3/2} + \Gamma n_{1/2} \qquad \text{(B-1b)}$$

where

$$S = 2\chi^2 \tilde{\gamma}_{12} \Delta^{-2} u^{-1} W_o(v/u) N_o \qquad \text{(B-1c)}$$

represents the pump field excitation of the $P_{1/2}$ state, and Γ and Γ' are the $1/2 \rightarrow 3/2$ and $3/2 \rightarrow 1/2$ collision rates, respectively. Equations (B-1) reflect the fact that only the $P_{1/2}$ state is significantly pumped by the field. All effects of velocity-changing collisions are neglected in the large detuning limit, since the intermediate state velocity distribution is Maxwellian. Solving Eq. (B-1b) for $n_{3/2}$ and substituting it into Eq. (B-1a) one obtains the steady-state equation for $n_{1/2}$

$$0 = -\gamma_{2eff} n_{1/2} + S \quad . \qquad \text{(B-2)}$$

where

$$\gamma_{2eff} = \gamma_2 \left(\frac{\gamma_2 + \Gamma' + \Gamma}{\gamma_2 + \Gamma'} \right) \quad . \qquad \text{(B-3)}$$

Thus, the net effect of the $P_{3/2}$ state can be included by replacing the decay rate γ_2 of the $P_{1/2}$ level by the $\gamma_2$eff of Eq. (B-3). For the $P_{1/2} - P_{3/2}$ levels, $\Gamma = 2\Gamma' \equiv \gamma_t$.

TABLE I

Broadening Coefficients (MHz/Torr) at 200°C

Perturber	$\frac{1}{2\pi}\left(\frac{d\tilde{\gamma}_{12}}{dP}\right)$	$\frac{1}{2\pi}\left(\frac{d\tilde{\gamma}_{23}}{dP}\right)$	$\frac{1}{2\pi}\left(\frac{d\tilde{\gamma}_{13}}{dP}\right)$	$\frac{1}{2\pi}\left(\frac{d\gamma_t}{dP}\right)$
He	6.2[a]	21.[c]	23.[d]	6.0[e]
Ne	3.7[a]	11.[c]	13.[d]	2.4[e]
Kr	12.[b]	27.[c]	29.[d]	2.7[e]

$\gamma_2/2\pi = 10$ MHz; $\gamma_3/2\pi = 3.2$ MHz; $\gamma_1/2\pi = 0.0$ MHz

$\tilde{\gamma}_{ij} = (\gamma_i + \gamma_j)/2 + \frac{d\tilde{\gamma}_{ij}}{dP} P$

a. D. G. McCartan and J. M. Farr, J. Phys. B. 9 985 (1976).

b. This work.

c. J. F. Kielkopf and R. B. Knollenberg, Phys. Rev. A 12 559 (1975).

d. F. Biraben, B. Cagnac, E. Giacobino, G. J. Phys. B. 10 2369 (1977).

e. Ref. 15.

REFERENCES

1. D. L. Huber, Phys. Rev. 178, 93 (1969).
2. A. Omont, E. W. Smith and J. Cooper, Astrophys. J. 175, 185 (1972).
3. J. L. Carlsten and A. Szöke, Phys. Rev. Lett. 36, 667 (1976) and J. Phys. B 9, L231 (1976).
4. J. L. Carlsten, A. Szöke and M. G. Raymer, Phys. Rev. A 15, 1029 (1977).
5. D. L. Rousseau, G. D. Patterson and P. F. Williams, Phys. Rev. Lett. 34, 1306 (1975).
6. R. D. Driver and J. L. Snider, J. Phys. B 10, 595 (1977).
7. D. Mihalas, Stellar Atmospheres (Freeman, San Francisco 1970) Chap. 10.
8. C. Brechignac, R. Vetter and P. R. Berman, Phys. Rev. A 17, 1609 (1978).
9. P. F. Liao, J. E. Bjorkholm and P. R. Berman, to be published.
10. P. R. Berman, Advances in Atomic and Mol. Phys. 13, 57 (1977).
11. D. Grischkowsky, Phys. Rev. A 14, 802 (1976).
12. J. E. Bjorkholm and P. F. Liao, Phys. Rev. Lett. 33, 128 (1974); Phys. Rev. A 14, 751 (1976).
13. E. Courtens and A. Szöke, Phys. Rev. A 15, 1588 (1977).
14. The same constant of proportionality is used in equations (1) and (2) because coherence effects are negligible. For other excitation polarizations and smaller detunings these constants may become functions of Δ and differ from each other - see for example, B. R. Marx and L. Allen, J. Phys. B 11, 3023 (1978).
15. J. C. Gay and W. B. Schneider, Zeit. F. Physik A 278, 211 (1976).
16. J. Apt and D. E. Pritchard, J. Phys. B 12, 83 (1979).
17. J. Cooper and R. J. Ballagh, Phys. Rev. A 18, 1302 (1978).

Figure Captions

Fig. 1 - Two-photon excitation spectra of the sodium $3S_{1/2} - 4D_{3/2}$ transition at various pressures of neon perturber gas. The detuning of the fixed frequency laser from intermediate state resonance is $\Delta/2\pi = -4.0$ GHz. The broad resonance is centered near the $3P_{1/2} \rightarrow 4D_{3/2}$ transition frequency. All spectra taken with the same detection sensitivity. Solid line - experimental curve; points - theory.

Fig. 2 - Comparison of experimental excitation spectra with theoretical lineshape that neglects fine-structure state-changing collisions in the 3P states.

Fig. 3 - Same as Fig. 1 except with helium and krypton perturbers. Detection sensitivity differs for these curves.

Fig. 4 - Amplitude of collisional redistribution signal vs. detuning, Δ. Points - experimental data; solid line - theory. Data taken with 10 Torr of neon buffer gas.

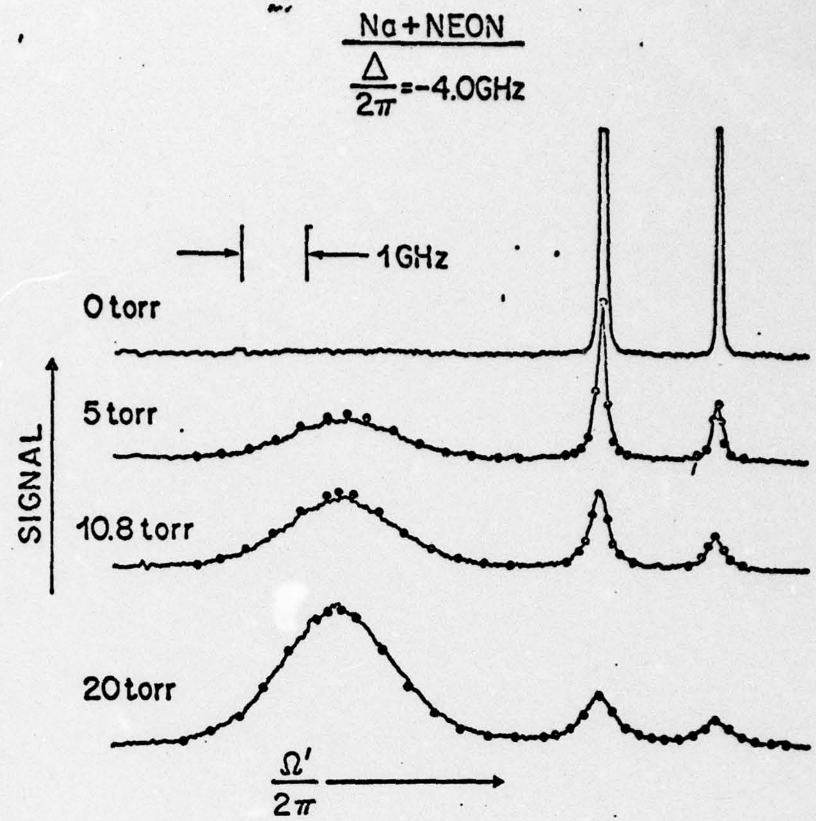

Fig. 1

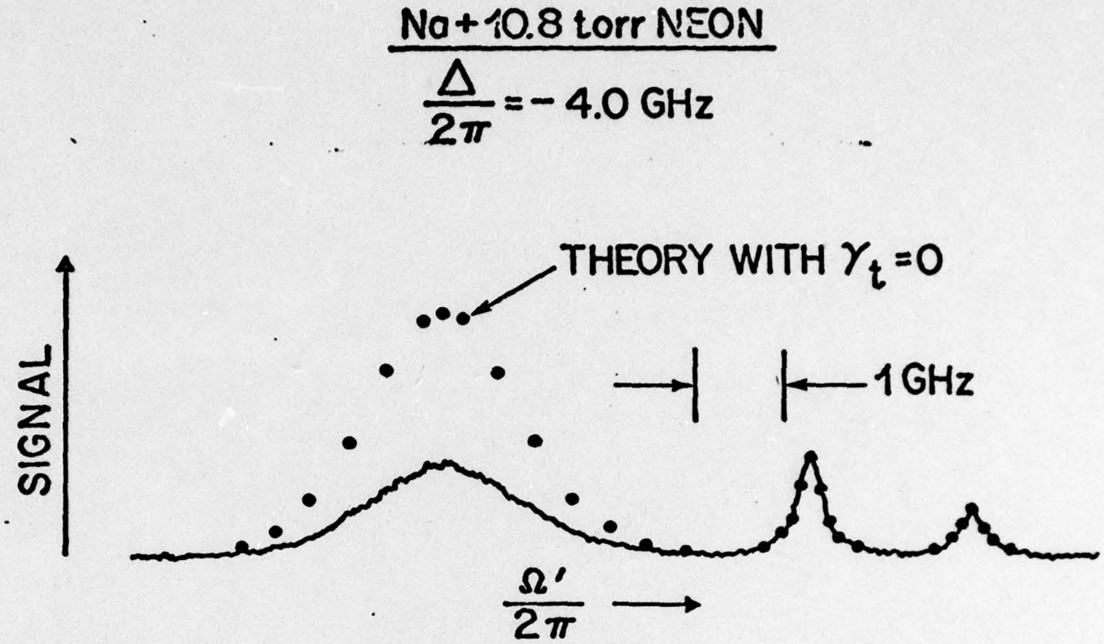
Na + 10.8 torr NEON
$\frac{\Delta}{2\pi}$ = − 4.0 GHz
THEORY WITH γ_t = 0
1 GHz
SIGNAL
$\frac{\Omega'}{2\pi}$

Fig. 2

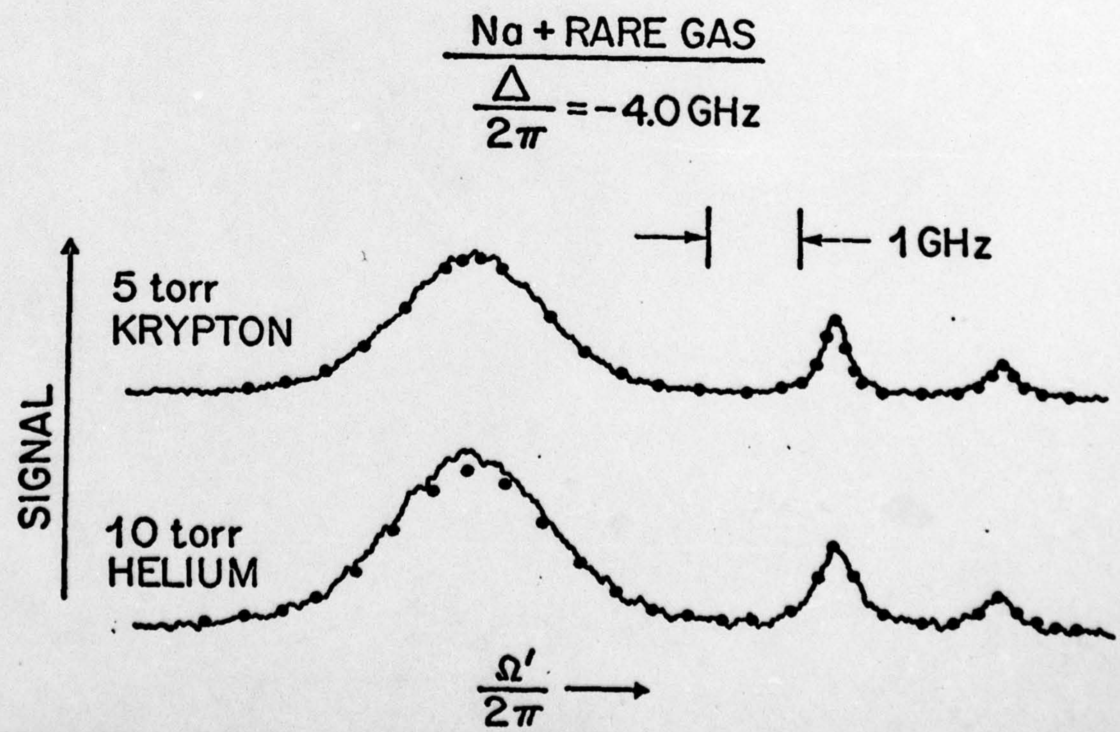
Na + RARE GAS
$\frac{\Delta}{2\pi}$ = − 4.0 GHz
1 GHz
5 torr KRYPTON
SIGNAL
10 torr HELIUM
$\frac{\Omega'}{2\pi}$

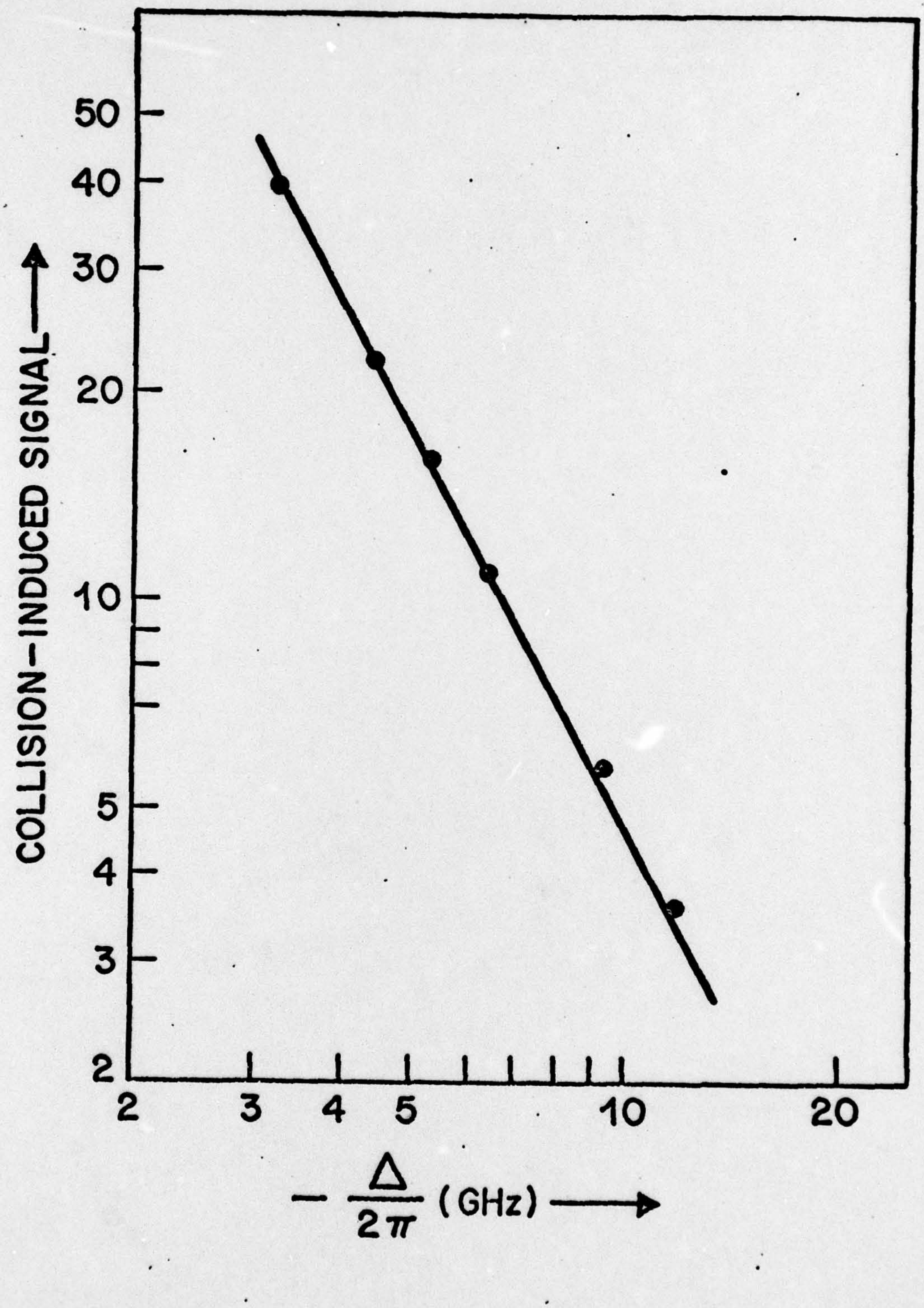

COLLISION-INDUCED SIGNAL
50
40
30
20
10
5
4
3
2
2
3
4
5
10
20
$-\frac{\Delta}{2\pi}$ (GHz)

Fig. 4